RESEARCH INTO ADVANCED CONCEPTS OF MICROWAVE POWER AMPLIFICATION AND GENERATION UTILIZING LINEAR BEAM DEVICES

P. R. McIsaac

School of Electrical Engineering

Cornell University

Semiannual Status Report

December 1970

Research Grant NGL 33-010-047 No. 2

National Aeronautics and Space Administration

Office of Grants and Research Contracts
Code SC
Washington, D. C. 20546

ABSTRACT

This is an interim report which summarizes work during the past six months on a theoretical study of some aspects of the interaction between a drifting stream of electrons with transverse cyclotron motions and an electromagnetic field. Particular emphasis is given to the possible generation and amplification of millimeter waves. This report includes a discussion of two aspects of the theory of cyclotron resonance oscillators. First, the start oscillation conditions for a cyclotron resonance oscillator are discussed using the results of digital computer calculations based on a small signal, coupled mode theory of the device. Second, the formulation of a large signal analysis of the cyclotron resonance oscillator to explore those factors which determine the saturation power output and efficiency is discussed.

TABLE OF CONTENTS

I. INTRODUCTION

The objective of this research program is to explore theoretically some aspects of the interaction between a drifting stream of electrons having transverse cyclotron motions and an electromagnetic field; particular emphasis being given to the possible generation and amplification of millimeter waves. Because of the interest in possible applications to millimeter wavelengths, this study concentrates on electron stream-electromagnetic field interactions which involve an uniform, or fast-wave, circuit structure or a cavity of simple shape.

This report discusses two aspects of the theory of the cyclotron resonance oscillator based on the model of a spiraling filamentary electron beam drifting through a rectangular cavity of square cross section. In Section II, the start oscillation conditions for the cyclotron resonance oscillator are summarized. This discussion is based on a small signal, coupled mode analysis[1,6] and presents results of fairly extensive calculations. Section II is essentially the text of a paper, "Start Oscillation Conditions for Cyclotron Resonance Oscillators," by P. R. McIsaac and J. F. Rowe, Jr., which was presented at the Eighth International Conference on Microwave and Optical Generation and Amplification, September 1970, in Amsterdam (MOGA 70).

Section III discusses some aspects of the formulation of a large signal analysis of the saturation effects in cyclotron resonance oscillators. A digital computer program has been developed to provide numerical results for typical parameter values for the

cyclotron resonance oscillator in order to explore those factors which determine the saturation of the power output and the resulting oscillator efficiency.

II. START OSCILLATION CONDITIONS FOR CYCLOTRON RESONANCE OSCILLATORS*

A. Introduction

The cyclotron resonance oscillator utilizes the interaction between the electromagnetic fields of a cavity and a spiraling electron beam drifting through the cavity along a longitudinal magnetic field. The interaction can produce an oscillation at a frequency close to the relativistic cyclotron frequency of the electrons. This paper describes the use of a small signal, coupled mode analysis to determine the start oscillation conditions for the cyclotron resonance oscillator. The dependence of the start oscillation beam current on the loaded Q and dimensions of the cavity, and on the d-c magnetic flux density B_o is discussed for typical beam and cavity parameters.

The model employed for this analysis assumes a spiraling filamentary electron beam drifting through a rectangular cavity of square cross section (height = width = a) with its length L adjusted so that the TE_{101} resonant frequency is close to the cyclotron frequency. Relativistic effects are included in the analysis; that is, magnetic as well as electric forces on the electrons are considered, and dependence of the electron mass on the velocity is included. Space charge forces are neglected. For the physical details of experimental cyclotron resonance oscillators, reference may be made to the literature.[2,3,4,5]

B. Coupled Mode Theory

A coupled mode theory for the interaction between a spiraling filamentary electron beam and the electromagnetic fields of an uniform waveguide was reported previously.[6] The circuit has four waves

*Text of paper presented at Eighth International Conference on Microwave and Optical Generation and Amplification, September 1970, Amsterdam.

(positive and negative circularly polarized waves in both the forward and reverse directions), while the electron beam has six waves. The beam waves can be labeled by their characteristic form in the limiting case of a straight filamentary electron beam: two cyclotron waves, two synchronous waves, and two (degenerate) space charge waves. It was found that significant interaction occurs between six of these waves; the forward and reverse, positive circularly polarized, circuit waves, and the two cyclotron and two degenerate space charge waves of the electron beam.

Figure 1 shows the ω-β diagram for these six waves in the coupled system. It should be noted that the curves for the two circuit waves and the two cyclotron waves have been shifted horizontally by $n\beta_c$; this simplifies the form of the coupled mode equations and their solutions in the spiraling electron beam case. Here, $n = (1 - (v_o/c)^2)^{\frac{1}{2}}$ and $\beta_c = \omega_c/v_{oz}$, where $\omega_c = eB_o/m_o$ is the non-realistic cyclotron frequency. Note that there is a pair of waves with complex conjugate propagation constants in the coupled system at both the lower and upper intersection points of the uncoupled system. However, it is found that amplification or oscillation occurs only in the neighborhood of the upper intersection point. The start oscillation calculations are based on this coupled mode theory which is applied to the one-port amplifier shown in Figure 2. The interaction space is a half wavelength cavity shorted at the right, through which the spiraling electron beam drifts from left to right. On the left, an input wave F'_{+i} which is positive circularly polarized relative to B_o is incident on the interaction region, and the output circuit wave G'_{+o}, also positive circularly polarized reltaive to B_o, propogates to the left. The various circuit and beam parameters are adjusted until

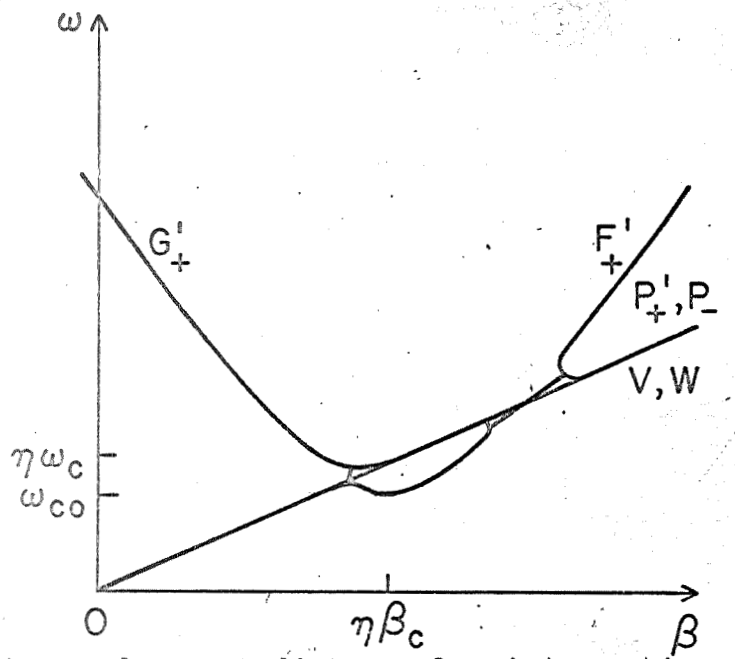

Figure 1. ω-β diagram for interaction between a spiraling filamentary electron beam and a waveguide. F'_+, G'_+ are positive circularly polarized circuit waves; P'_+, P'_- are beam cyclotron waves; V, W are beam (degenerate) space charge waves.

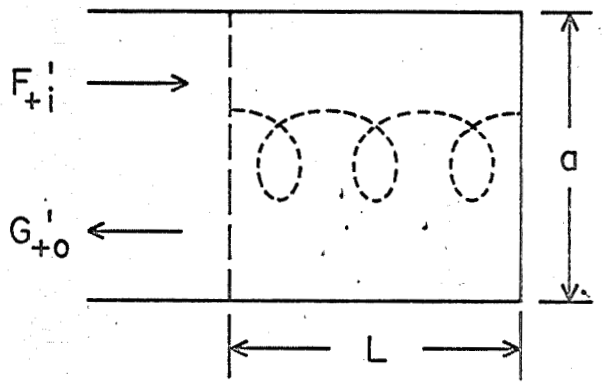

Figure 2. Schematic Diagram of a cyclotron resonance oscillator.

the amplifier gain G'_{+o}/F'_{+i} is infinite; this determines the start oscillation condition.

The electron beam parameters are the normalized axial and transverse velocities, $\sigma = v_{oz}/c$ and $\zeta = \eta\omega_c r_o/c$ (where r_o is the d-c beam radius), and the d-c beam current I_o. The cavity parameters, in addition to L and a, are Q_o, Q_x, and Q_L. Losses in the cavity walls are included, with Q_o adjusted to account for copper walls. In this model Q_x is varied by changing the assumed characteristic impedance of the output waveguide.

The general form for the solution of six coupled mode equations is known. For a given set of parameter values, a digital computer is used to evaluate the propagation constants for the coupled waves (in the neighborhood of the upper intersection point on the ω-β diagram) and to evaluate the wave amplitudes and phases which are fixed by the boundary conditions. Then the computer calculates the gain G'_{+o}/F'_{+i}, for the one-port amplifier. The parameter values that must be chosen are σ, ζ, a (or f_{co}), Q_o, ηf_c, L and I_o. For each set of these parameters, pairs of values for Q_x and the start oscillation frequency f_{so} are successively guessed and the gain is calculated. When a pole in the gain is achieved (in practice a gain in excess of 100 is accepted), the set of parameter values is taken to be the start oscillation condition. Although this is trial-and-error procedure, the parameter range for oscillation is limited, and experience enables start oscillation conditions to be attained within a few tries. Thus, in practice the procedure is rapid and not expensive in computer time.

For a given value of the d-c magnetic field there is only a limited range of cavity length which will produce oscillation. It is

possible to optimize the combination of nf_c and L for fixed values of the other parameters to produce start oscillation for the minimum Q_L. In general, this optimization was not attempted in this investigation. Most of the calculations were made with a cavity length L such that the cavity TE_{101} resonance occurred at a frequency $f_o = 1.01\ f_c$. However, it became apparent in the study that a more optimum value would have been with L such that $f_o = 1.005\ nf_c$, and some data were taken with this value.

All of the data presented in Figures 3 through 7 are for $\sigma = 0.01$, $\zeta = 0.20$, and $f_{co} = 9$ GHz (a = 1.6655 cm).

C. Start Oscillation Conditions

Figure 3 shows the start oscillation beam current I_o versus Q_L with L/a as a parameter for $f_o = 1.01\ nf_c$. Note that the various curves are nearly straight lines. It is found that in the range $0.9 < L/a < 1.5$, I_o varies approximately as $1/Q_L$ in agreement with experiment.[5] For $L/a < 0.9$, I_o decreases more rapidly, and for $L/a > 1.5$, I_o decreases more slowly than $1/Q_L$. Limited calculations of I_o versus Q_L for a cavity with $f_{co} = 90$ GHz gave results which coincided with the curves shown for $f_{co} = 9$ GHz. It is presumed that the results obtained here can be scaled throughout the microwave and millimeter wavelength range.

The influence of the axial velocity parameter σ was briefly examined. For $I_o = 1.0$ mA, $L/a = 2.2$, and $\zeta = 0.20$, calculations for $\sigma = 0.02$ and 0.03 were made. It was found that for $\sigma = 0.02$, the start oscillation Q_L was increased by a factor of five, while for $\sigma = 0.03$, no start oscillation condition could be achieved. Thus, we conclude that the start oscillation conditions are a sensitive

function of the axial drift velocity.

Figure 4 shows the start oscillation current I_o versus Q_L for the same beam and cavity parameters as Figure 3, but with $f_o = 1.005\ nf_c$. Note that the general shape of the curves is similar to the previous figure, but the curves are shifted to lower values of Q_L. These curves, together with other calculations, indicate that this combination of L/a and nf_c is nearly optimum.

For reference, Figure 5 shows the variation of the start oscillation frequency with cavity length, plotting f_{so}/f_{co} versus L/a. This curve is only approximate, since there is some frequency pushing as I_o is varied, and also the oscillation frequency shifts slightly as nf_c is varied at fixed L/a. However, these effects are negligible on the scale of this figure. Note that start oscillation calculations have been made over a frequency range of about three to one.

Figure 6 shows curves of L/a versus Q_L at start oscillation with the d-c beam current I_o as the parameter for $f_o = 1.01\ nf_c$. For $I_o \lesssim 0.5$ mA, there is an optimum value for L/a for which the Q_L at start oscillation is minimum. For $I_o = 0.1$ mA, start oscillation conditions are obtained only for $0.5 \lesssim L/a \lesssim 3$. For $I_o \gtrsim 0.8$ mA, there is apparently no optimum value for L/a, and as L/a is increased, Q_L for start oscillation decreases monotonically. Thus at a d-c beam current between 0.5 and 0.8 mA, the character of the curves changes.

Figure 7 shows curves of L/a versus Q_L at start oscillation for $f_o = 1.005\ nf_c$. Note that these curves are shifted upward toward higher values of Q_L compared to the curves in Figure 6. This again indicates that this combination of L/a and nf_c is more nearly optimum for start oscillation of the cyclotron resonance oscillator at a given d-c beam current.

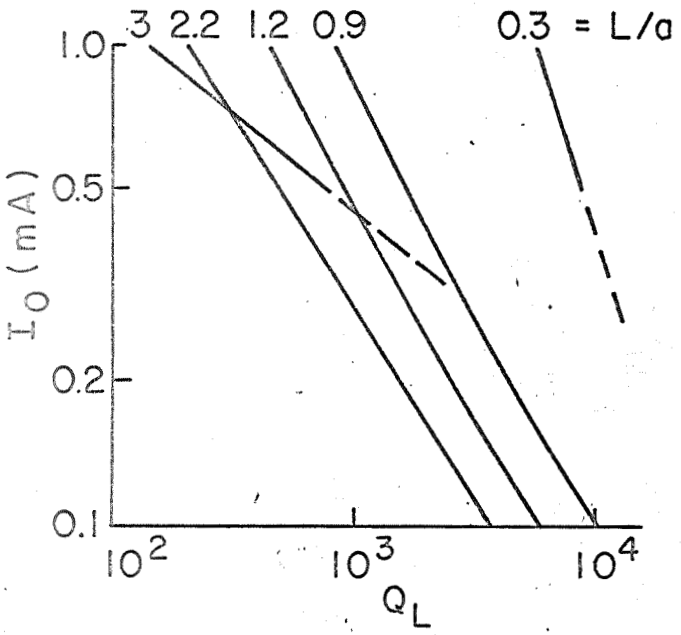

Figure 3. Start oscillation d-c beam current I_o versus Q_L (f_o = 1.01 nf_c).

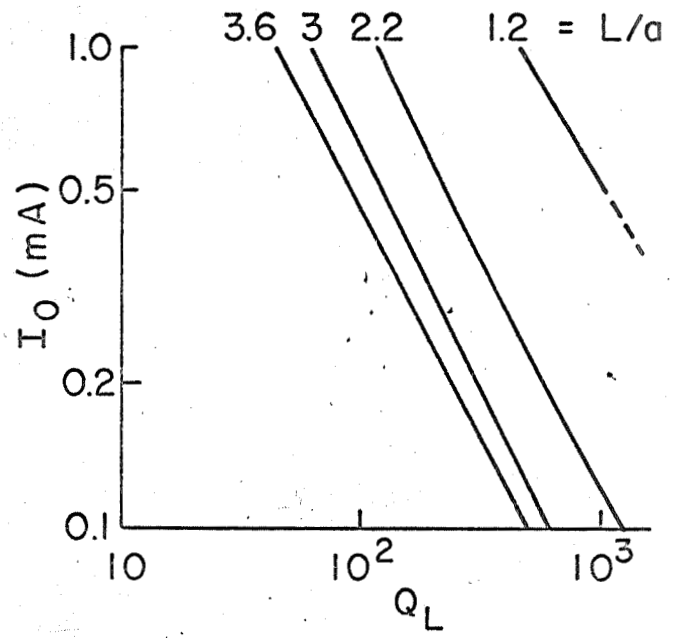

Figure 4. Start oscillation d-c beam current I_o versus Q_L (f_o = 1.005nf_c).

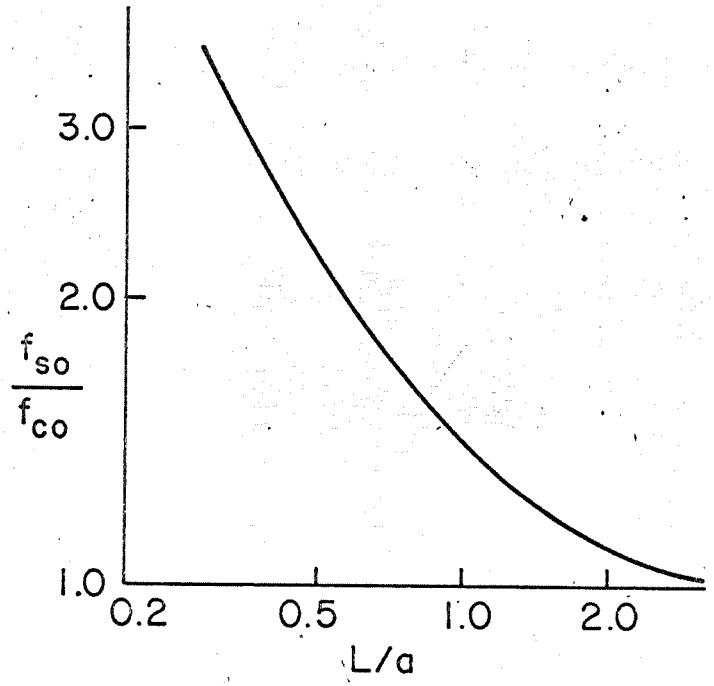

Figure 5. Ratio of start oscillation frequency to waveguide cutoff frequency, f_{so}/f_{co}, versus ratio of cavity length to width, L/a.

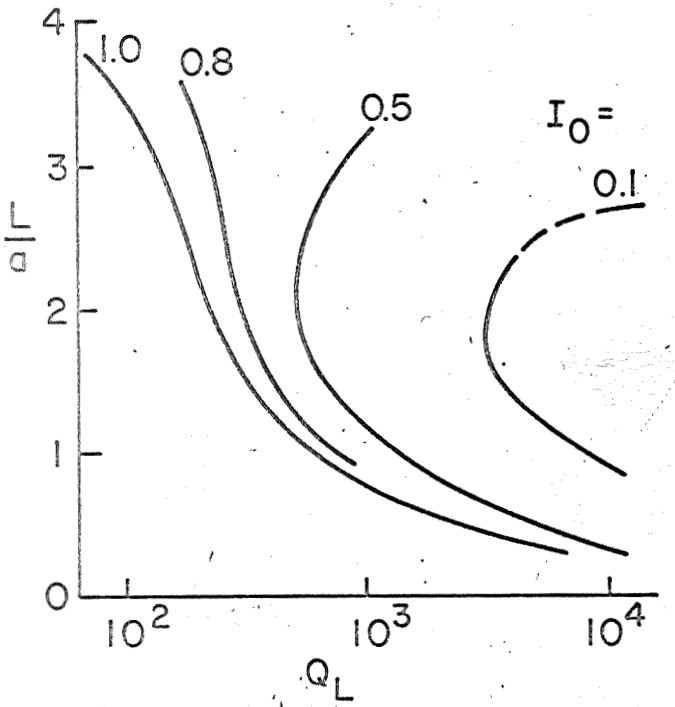

Figure 6. Ratio of cavity length to width, L/a, versus Q_L, at start oscillation ($f_o = 1.01nf_c$).

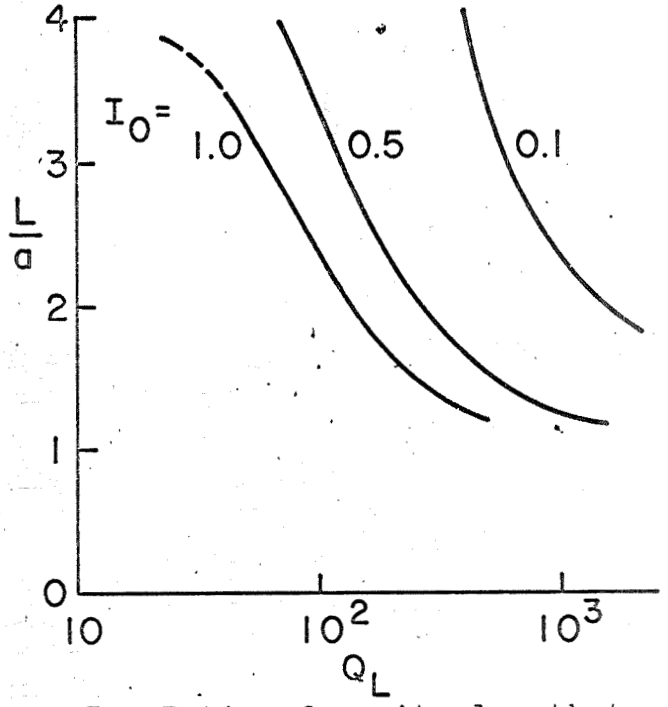

Figure 7. Ratio of cavity length to width, L/a, versus Q_L at start oscillation ($f_o = 1.005nf_c$).

All the curves in Figure 7 show a monotonic decrease of Q_L as L/a is increased. That is, no optimum value of L/a exists, at least for $0.1 \leq I_o \leq 1.0$ mA, and these curves are all similar to the curves in Figure 6 for the larger beam currents $I_o \gtrsim 0.8$ mA. This suggests that the change in the character of the curves in Figure 6 as the d-c beam current is decreased is caused by the non-optimum combination of L/a and ηf_c. For the optimum combination of L/a and ηf_c, start oscillation can presumably be achieved down to low values of Q_L for low values of d-c beam current by increasing L/a; that is, by operating close to the cutoff frequency f_{co} of the waveguide. Reference to the coupled mode theory[6] shows that the coupling parameter involves the waveguide impedance which approaches infinity at f_{co} for TE modes. However, if the combination of L/a and ηf_c is not optimum, then the range of beam currents for which start oscillation at low values of Q_L can be achieved is limited. In this case one finds a beam current level below which only a minimum value of Q_L can be obtained at a finite value of L/a, as shown by the curves in Figure 6 for $I_o \lesssim 0.5$ mA. There is some indication that the start oscillation conditions may change for very large values of L/a, but this has not yet been explored.

The sensitivity of the start oscillation frequency to the d-c beam current can be determined by comparing the start oscillation frequency f_{so} to the upper intersection frequency f_u on the ω-β diagram for the beam-circuit system in the limit of zero coupling. It is found that for the optimum combination of L/a and ηf_c (i.e., $f_c = 1.005\ \eta f_c$), $|\Delta f| \lesssim 0.002\ f_u$, where $\Delta f = f_{so} - f_u$. For large values of L/a (e.g., L/a $\gtrsim$ 3), Δf is positive and decreases with increasing

beam current. For smaller values of L/a, Δf increases with increasing beam current; in this range Δf is positive for moderate values of L/a and negative for small values (e.g., L/a $\lesssim$ 1.5). It is estimated that a value of L/a between 2.5 and 3 will produce a start oscillation frequency that is approximately independent of the d-c beam current in the range from 0.1 to 1.0 mA.

III. LARGE SIGNAL ANALYSIS OF THE CYCLOTRON RESONANCE OSCILLATOR

A. Oscillator Model and Assumptions

The model of the cyclotron resonance oscillator adopted for the large signal analysis is similar to the one used for the small signal analysis of the start oscillation conditions. A spiraling filamentary electron beam is assumed to drift through a rectangular cavity of square cross section. The oscillator output is taken at the cavity end where the electron beam enters (see Figure 2). Several of the simplifying assumptions that have been made are listed below.

1. The cavity walls are perfectly conducting, so the cavity is lossless.
2. The electron beam is filamentary, and space charge forces are neglected.
3. The electron beam is assumed to be mono-velocity at any cross section (although both the d-c and a-c beam velocity may vary axially along the interaction cavity).
4. The electron beam orbiting radius is much less than the cavity transverse dimension.
5. The transverse electromagnetic fields in the cavity, both homogeneous and inhomogeneous components, are assumed to vary sinusoidally across the cavity, and only interaction with the lowest resonant mode of the cavity is considered.

Within the interaction cavity, the basic equations for the system are:

$$\nabla^2\bar{E} - \frac{1}{c^2}\frac{\partial^2\bar{E}}{\partial t^2} = \frac{\nabla\rho}{\varepsilon_o} + \mu_o\frac{\partial\bar{J}}{\partial t} \quad , \tag{1}$$

$$\nabla^2\bar{H} - \frac{1}{c^2}\frac{\partial^2\bar{H}}{\partial t^2} = -\nabla x\bar{J}, \qquad (2)$$

$$\frac{d}{dt}\left\{\frac{\bar{v}}{(1 - v^2/c^2)^{1/2}}\right\} = -\frac{e}{m_o}\left[\bar{E} + \mu_o\bar{v}x\bar{H} + \mu_o\bar{v}x\bar{H}_o\right]. \qquad (3)$$

Here, $\bar{E}$ and $\bar{H}$ are the a-c electromagnetic fields of the interaction cavity, H_o is the axial d-c magnetic field which determines the electron beam cyclotron frequency, ρ and $\bar{J}$ are the electron beam charge and current densities, and $\bar{v}$ is the electron beam velocity. Note that relativistic effects are included in Equation (3); m_o is the electron rest mass and e is the magnitude of the electron charge. The boundary conditions for the system are the following: a) the electron beam enters the interaction cavity unmodulated (the a-c values of ρ, $\bar{J}$, and $\bar{v}$ are zero at the electron beam input), b) the tangential electric field at the collector end of the cavity is zero, and c) the transverse values of the electric and magnetic fields at the cavity output (the cavity end where the electron beam enters) must be consistent with the power output of the oscillator.

To solve the equations for the electron beam - cavity interaction, it is assumed that the oscillator has reached a steady state, and that the oscillator output consists of a periodic signal composed of a strong fundamental frequency component (close to the cavity resonant frequency and the electron beam cyclotron frequency) plus the harmonics of the fundamental frequency. A digital computer is used to integrate the equation of motion, Equation (3), through the interaction cavity from the electron beam input to the collector. Since this integration is done numerically in finite steps, the electron beam is decomposed into a series of discrete charge groups,

and eight charge groups per r-f cycle have been used. It was found that in order to obtain a stable solution, the axial step length along the cavity for the integration must be a small fraction of the electron beam d-c helix pitch. For a step length corresponding to 1/800 of the d-c helix pitch the electron beam was found to be stable indefinitely, and the cumulative error in the d-c beam parameters for no r-f interaction was about 0.1% for a total length of 40 d-c beam cycles (this corresponds to the typical cyclotron resonance oscillator length). Increases in step size resulted in rapid error growth. It is anticipated that all computing runs will be done with this step length of 800 per d-c beam cycle.

To solve the equations for the electromagnetic fields, Equations (1) and (2), the fields are expressed as a Fourier series consisting of the fundamental oscillation frequency and its harmonics. Further, the fields are divided into two parts: the homogeneous fields (at the fundamental frequency only) which are solutions to the homogeneous part of Equations (1) and (2) and represent the ordinary standing-wave fields for the lowest cavity resonant mode; and the inhomogeneous fields (these include components at the fundamental frequency and its harmonics) which are the solution to the inhomogeneous parts of Equations (1) and (2) with the electron beam charge and current densities as the driving terms.

The solution procedure can be described qualitatively in the following way. The spiraling electron beam enters the cavity and is acted on by the homogeneous r-f electromagnetic fields. As a result, the electron beam becomes distorted in form as position modulation appears. A Fourier analysis of the beam variables is performed at

periodically spaced axial intervals, and based on certain "slowly varying" assumptions on the Fourier coefficients, approximate closed-form expressions for the inhomogeneous fields can be generated. These fields are fed back into the equations of motion for the charge groups so that they can be integrated along the length of the cavity.

An initial guess must be made of the oscillator power output and the fundamental oscillation frequency for a given set of electron beam and cavity parameters. If this guess is correct, then the solution procedure will yield an axial location (about a half wavelength along the cavity) at which the homogeneous electric field and the inhomogeneous electric field combine to give a null. At this location, then, the collector end wall of the cavity may be placed, and the boundary conditions satisfied.

B. Computer Program Flow Diagram

The computer program flow diagram is shown in Figure 8. In order to minimize the running time for the program, the inhomogeneous electromagnetic field coefficients are not adjusted at each axial integration step. Rather, they are updated once each d-c electron beam cycle. This is justified by the observed result that for all the parameters tried so far, the inhomogeneous fields are much smaller than the homogeneous fields over all the cavity length except for the region adjacent to the collector wall. Therefore, small errors in the inhomogeneous fields used for integrating the equations of motion for the charge groups will produce little error in the solution.

The electron beam and cavity parameters to be investigated have been chosen to approximate those used by Kulke in his experimental cyclotron resonance oscillator.[7] These parameters are listed in Table 1.

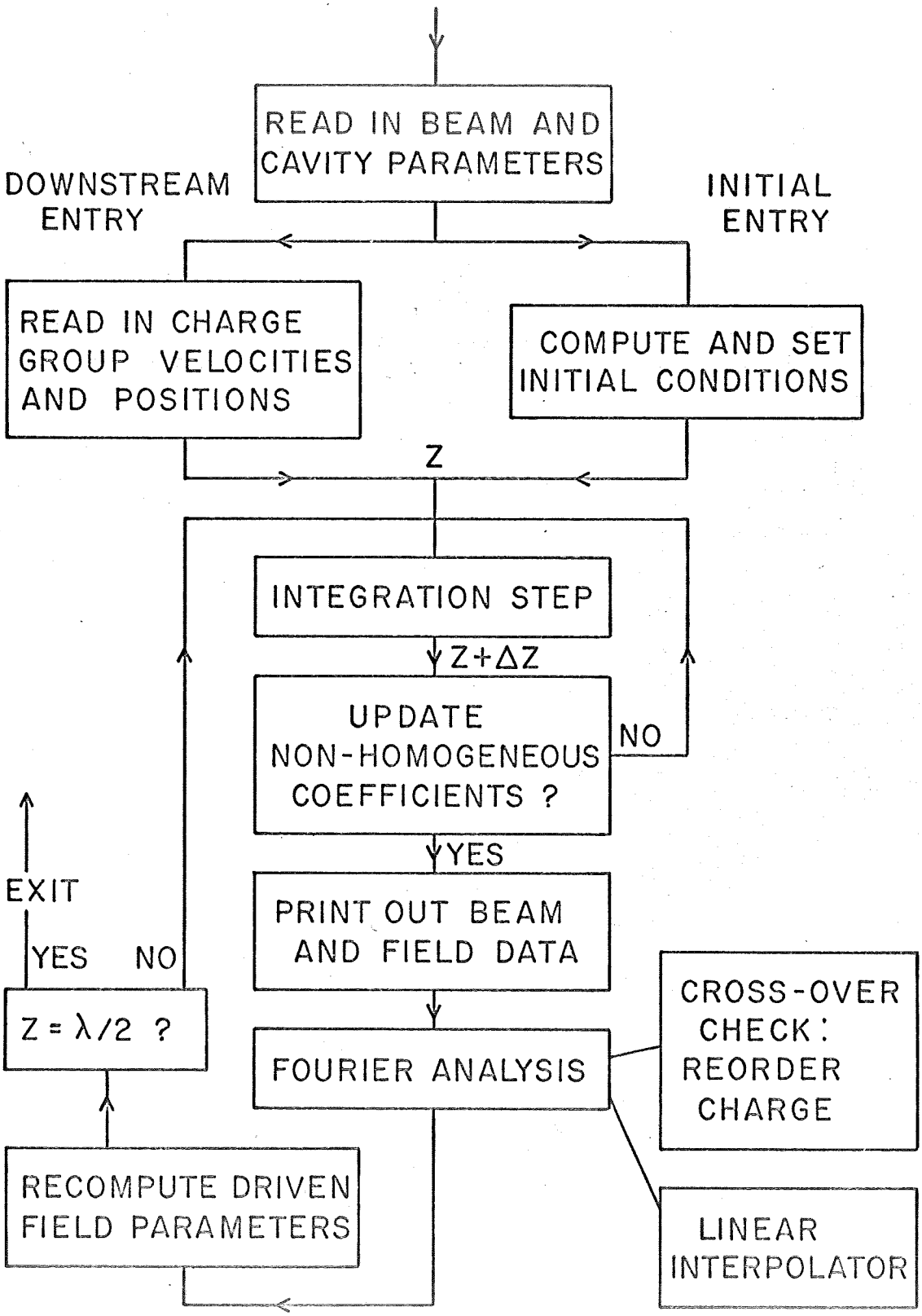

Figure 8. Computer program flow diagram.

TABLE 1. Cavity and Electron Beam Parameters

Cavity:	length = 2.14 cm
	cross section = 2.29 × 2.29 cm
Beam:	d-c current = 5.5 mA
	axial drift velocity = 0.01813c (84 volts axial energy)
	transverse velocity = 0.2356c (15 kilovolts transverse energy)
	axial magnetic field = 3439 gauss
	orbiting frequency = 9.352 GHz
	orbiting radius = 0.120 cm
	cavity length in d-c beam cycles = 37.75

REFERENCES

1. McIsaac, P. R.,Semiannual Status Report, NASA Research Grant NGR 33-010-047, Decmeber 1967, June 1968, December 1968, July 1969, and December 1969.
2. Hirshfeld, J. L. and Wachtel, J.M., "Electron Cyclotron Maser," Phys. Rev. Letters, 12, 1964.
3. Bott, I. B., "A Powerful Source of Millimetre Wavelength Electromagnetic Radiation," Physics Letters, 14, 293, 1965.
4. Beasley, J. P., "An Electron Cyclotron Resonance Oscillator at Millimetre Wavelengths," Proc. 6th Int. Conf. on Microwave and Optical Generation and Amplification, 132, Cambridge, 1966.
5. Kulke, B. and Wilmarth, R. W., "Small-Signal and Saturation Characteristics of an X-Band Cyclotron-Resonance Oscillator," Proc. IEEE, 57, 219, 1969.
6. McIsaac, P. R., "Spiraling Electron Beam Interaction with Fast Wave Circuits," Proc. 7th Int. Conf. on Microwave and Optical Generation and Amplification, 253, Hamburg, 1968.
7. Kulke, B., "Design Considerations for Cyclotron Resonance Oscillators," Technical Note D-5237, (June 1969), NASA, Electronics Research Center, Cambridge, Mass.